REPORT DOCUMENTATION PAGE

Form Approved
OMB No. 0704-0188

1. REPORT DATE *(DD-MM-YYYY)*	2. REPORT TYPE	3. DATES COVERED *(From - To)*
08-09-2010	Fellowship Program Final Report	

4. TITLE AND SUBTITLE

Identification of Coherent Structure Dynamics in Wall-Bounded Sprays using Proper Orthogonal Decomposition

5a. CONTRACT NUMBER

5b. GRANT NUMBER

5c. PROGRAM ELEMENT NUMBER

6. AUTHOR(S)
Vinod Narayanan & Benn Eilers (Oregon State University)

5d. PROJECT NUMBER

5f. WORK UNIT NUMBER
50260538

7. PERFORMING ORGANIZATION NAME(S) AND ADDRESS(ES)

Air Force Research Laboratory (AFMC)
AFRL/RZSA
10 E. Saturn Blvd.
Edwards AFB CA 93524-7680

8. PERFORMING ORGANIZATION REPORT NUMBER

AFRL-RZ-ED-TP-2010-373

9. SPONSORING / MONITORING AGENCY NAME(S) AND ADDRESS(ES)

Air Force Research Laboratory (AFMC)
AFRL/RZS
5 Pollux Drive
Edwards AFB CA 93524-7048

10. SPONSOR/MONITOR'S ACRONYM(S)

11. SPONSOR/MONITOR'S NUMBER(S)
AFRL-RZ-ED-TP-2010-373

12. DISTRIBUTION / AVAILABILITY STATEMENT

Approved for public release; distribution unlimited (PA #10446).

13. SUPPLEMENTARY NOTES
Air Force Summer Faculty Fellowship Program Final Report for submission to the American Society of Engineering Education (ASEE).

14. ABSTRACT

Wall interaction of sprays emanating from Gas Centered Swirl Coaxial (GCSC) injectors were experimentally studied as a part of this ten-week project. A key aspect of the work was to apply the Proper Orthogonal Decomposition (POD) method of data analysis to time-resolved intensity images of these sprays. A high-speed camera with backlighting was used to generate the intensity movies.

15. SUBJECT TERMS

16. SECURITY CLASSIFICATION OF:			17. LIMITATION OF ABSTRACT	18. NUMBER OF PAGES	19a. NAME OF RESPONSIBLE PERSON
a. REPORT	b. ABSTRACT	c. THIS PAGE			Dr. Stephen Danczyk
Unclassified	**Unclassified**	**Unclassified**	SAR	15	19b. TELEPHONE NUMBER *(include area code)* N/A

Air Force Summer Faculty Fellowship Program 2010

Final Report

Identification of Coherent Structure Dynamics in Wall-Bounded Sprays using Proper Orthogonal Decomposition

Prepared by

Vinod Narayanan

Associate Professor, Oregon State University

Benn Eilers

Graduate Student, Oregon State University

Submitted to

AFRL RZSA Edwards Air Force Base

and

American Society of Engineering Education (ASEE)

Dated

August 31st 2010

Abstract

Wall interaction of sprays emanating from Gas Centered Swirl Coaxial (GCSC) injectors were experimentally studied as a part of this ten-week project. A key aspect of the work was to apply the Proper Orthogonal Decomposition (POD) method of data analysis to time-resolved intensity images of these sprays. A high-speed camera with backlighting was used to generate the intensity movies.

Data were collected using three experimental test sections in a spray facility at Air Force Research Laboratories located at Edwards Air Force Base (AFRL/EAFB). The first facility consisted of a single acrylic GCSC injector with a transparent wall spaced at different locations relative to the injector. The second test section consisted of two injectors interacting with a single wall. The third test section consisted of the two injectors located within a chamber. Experiments were performed at atmospheric pressure using all three test sections. In addition, the chamber tests were also performed at elevated pressures of 6.8 bar and 20.4 bar. Approximately 200 experiments were performed and high-speed movies in excess of 2 terabytes were collected. Varied parameters included momentum flux ratios, injector-wall spacing, camera angle relative to the injectors and wall, and mass flow rate bias between the injectors for two-injector experiments.

Data of both raw intensity images and intensity fluctuations were subjected to POD analysis. For the raw intensity images, the first mode captured in excess of 98 percent of the intensity in the time-mean spray core. For most sprays, the first 8 modes were sufficient to represent the variations in left and right spray angles and attachment

points. In excess of 300 modes had to be reconstructed in order to capture the larger droplets emanating from the spray edges. Significantly large numbers of modes were needed to reconstruct the intensity fluctuation time series data that the raw intensity data.

The left and right spray angles, attachment point and jet width variations were used as primary indicators in a comparison of free sprays with wall-bounded sprays. Lower momentum-flux-ratio sprays indicated a larger variation in spray angle with time for free sprays and in the unbounded spray angle for wall-bounded sprays. Similarly, a larger variation in attachment locations was observed for lower momentum-flux-ratio sprays. Time variations of the wall-bounded spray angle are damped for closer wall spacing of 5 mm compared with the 10 mm spacing.

I. Introduction and Background

Recent studies at AFRL Edwards Air Force Base (AFRL/EAFB) have documented atomization characteristics of a Gas-Centered Swirl Coaxial (GCSC) injector [1-2], in which the oxidant is injected in a gaseous form in a central post and the fuel is introduced tangentially through holes at the periphery of the central post (see Fig. 1). The current 10-week project was aimed at documenting spray-wall interactions in these GCSC sprays. Specifically, two heretofore-unstudied aspects of GCSC injector sprays, illustrated in Fig. 1, were the focus of this project: (1) interaction of a GCSC spray with the chamber wall, and (2) effect of interaction between sprays from a wall-bounded injector and a main injector on the spray-wall interaction. A unique cold-flow facility at AFRL/EAFB was be used to document the GCSC injector spray-wall interactions. Nitrogen was used to simulate the oxidizer while water was used to simulate the liquid fuel. Time-resolved intensity maps were recorded using a high-speed camera with backlighting. Intensity maps were represented using a POD method and further

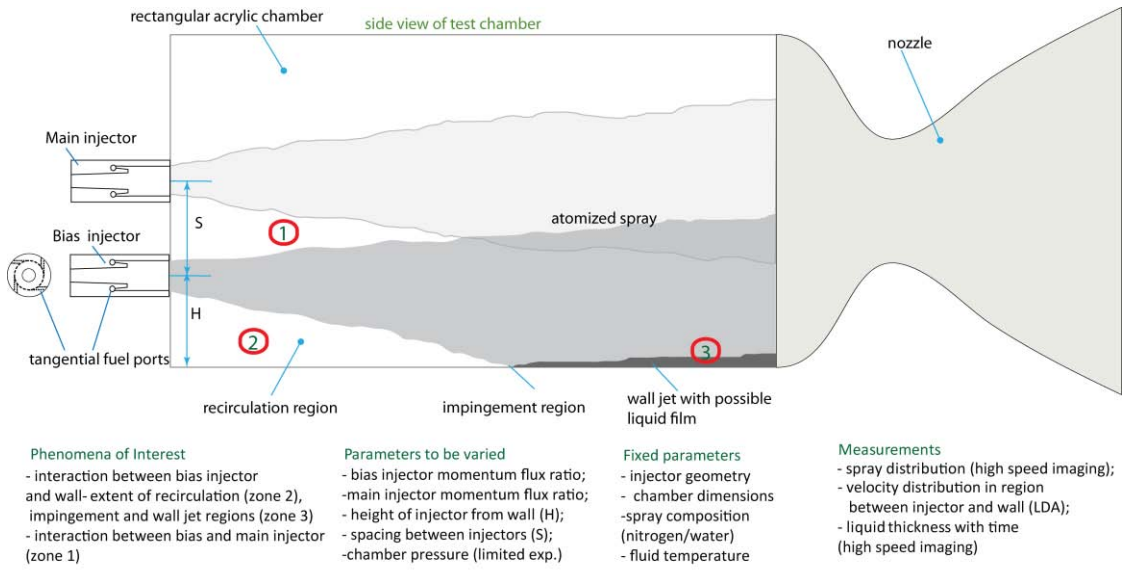

Fig. 1. Injector-wall Interaction – Parameters of Interest

analyzed to extract mean and time-varying information such as spray angles, attachment location and spray width variations.

II. Experimental facility

A simplified schematic of the flow facility at EAFB is shown in Fig. 2. Pressurized nitrogen at ~2400 psig was supplied to the flow lab. This nitrogen was regulated down to desired pressures and used to pump water from a tank to the test section. Nitrogen was also regulated separately in another line and sent to the test section. A sonic nozzle on the nitrogen line and a cavitating venturi on the water line were used to determine the mass flow rates in each stream. Pressure and temperature upstream of, and pressure downstream of, the flowmeters were recorded for use in nozzle and venturi equations. All pressure transducers were calibrated prior to the beginning of experiments with respect to a NIST traceable standard (Ruska Digital Pressure Calibrator). Pressures and temperatures were monitored using a Pacific Instruments data acquisition system and recorded manually. A Phantom v.7.3 high-speed camera was used to record movies with a spatial resolution of 800 x 600 pixels and an

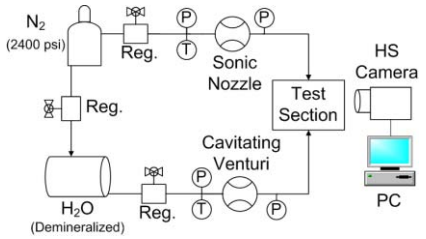

Fig. 2. Simplified schematic of experimental facility at AFRL/EAFB

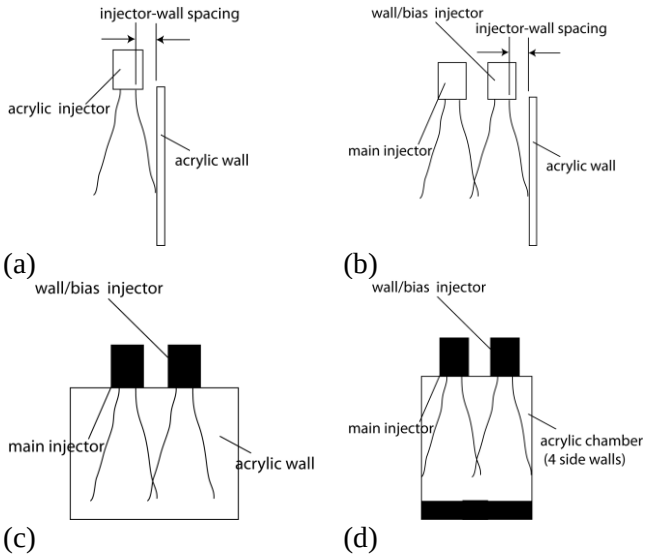

Fig. 3. Schematic of experimental test sections used depicting the orientation of spray and wall

acquisition rate of ~6700 frames per second for a typical duration of 1.5 seconds. A 250-watt halogen light source with a diffuser was used predominantly in a backlit configuration to illuminate the field of view of the spray.

Three test sections were used in this study with the aim of systematically analyzing spray-wall effects. The first one consisted of a single acrylic injector with an acrylic wall located either 1 mm, 5 mm, or 10 mm away from the edge of the injector and parallel to it (see Fig. 3a). The second test section consisted of two injectors with the wall oriented either near one injector (Fig. 3b) or equidistant from both injectors (Fig. 3c). The last test section consisted of an acrylic chamber that surrounded the two injectors in order to simulate injector operation within a combustion chamber of a rocket engine (Fig. 3d).

Table 1 summarizes the experimental matrices for tests performed using the first test section. Varied parameters for the first test section (Fig. 3a) included the momentum-flux-ratio (MFR), injector-to-surface spacing, and orientation of the camera relative to the injector and wall. For the second test section (see Tables 2 and 3), both biased and unbiased conditions were tested for the twin-injector configurations. For both of these test sections, free spray data were also recorded in order to provide a baseline for illustrating the effects of the sidewall on spray characteristics. In addition to MFR ratio variation and biasing, the chamber experiments were performed at pressures of 1 bar, 6.8 bar and 20.4 bar (Table 4).

Data Analysis and Typical Results

In excess of 2 terabytes of high-speed movies of spray intensities were recorded over all three test sections. Each movie file was in a binary file format (.cin format) and

Table 1. Single injector- free spray & wall test matrix

MR	Wall Spacing (mm)	Camera View of Wall
50	free spray	-
200	free spray	-
350	free spray	-
500	free spray	-
650	free spray	-
800	free spray	-
50	1, 5, 10	side & back
200	1, 5, 10	side & back
350	1, 5, 10	side & back
500	1, 5, 10	side & back
650	1, 5, 10	side & back
800	1, 5, 10	side & back
MR- Momentum flux ratio		

Table 2. Twin injectors- free spray matrix

MR*	Bias (%)	MR Scaling	Injector	Wall Spacing (mm)
50	0	V_{ax}, m_{H2O}	Main	free spray(s)
200	0	V_{ax}, m_{H2O}	Main	free spray(s)
350	0	V_{ax}, m_{H2O}	Main	free spray(s)
500	0	V_{ax}, m_{H2O}	Main	free spray(s)
650	0	V_{ax} , m_{H2O}	Main	free spray(s)
800	0	V_{ax}, m_{H2O}	Main	free spray(s)
50	0, 25	V_{ax}	Main+Bias	free spray(s)
200	0, 25	V_{ax}	Main+Bias	free spray(s)
350	0, 25	V_{ax}	Main+Bias	free spray(s)
500	0, 25	V_{ax}	Main+Bias	free spray(s)
650	0, 25	V_{ax}	Main+Bias	free spray(s)
800	0, 25	V_{ax}	Main+Bias	free spray(s)
*MR- based on unbiased injector				
Total number of runs: 24				

Table 3. Twin injectors-wall test matrix

MR*	Bias (%)	MR Scaling	Injector	Wall Spacing (mm)	Camera View of Wall
50	0, 25	Vax	Main+Bias, Main (for cam. view 2, 10 mm)	5, 10	1, 2 (for 10 mm), 3 (for 5 mm, 0 bias)
200	0, 25	Vax	Main+Bias, Main (for cam view 2, 10 mm)	5, 10	1, 2 (for 10 mm), 3 (for 5 mm, 0 bias)
350	0, 25	Vax	Main+Bias, Main (for cam view 2, 10 mm)	5, 10	1, 2 (for 10 mm), 3 (for 5 mm, 0 bias)
500	0, 25	Vax	Main+Bias, Main (for cam view 2, 10 mm)	5, 10	1, 2 (for 10 mm), 3 (for 5 mm, 0 bias)
650	0, 25	Vax	Main+Bias, Main (for cam view 2, 10 mm)	5, 10	1, 2 (for 10 mm), 3 (for 5 mm, 0 bias)
800	0, 25	Vax	Main+Bias, Main (for cam view 2, 10 mm)	5, 10	1, 2 (for 10 mm), 3 (for 5 mm, 0 bias)
1	wall near bias injector, camera side view of wall				
2	both injectors equidistant from the wall, camera has back view of wall				
3	bias injector near imaged wall, camera has back view of wall				
	Total number of runs: 52				

Table 4. Twin injectors- chamber test matrix

P_{ch} (psig)	MR*	Bias (%)	MR Scaling	Injector	Camera View of Wall
0	50	0, 25	V_{ax}	Main, Bias, Main+Bias	1, 2
0	200	0, 25	V_{ax}	Main, Bias, Main+Bias	1, 2
0	350	0, 25	V_{ax}	Main, Bias, Main+Bias	1, 2
0	500	0, 25	V_{ax}	Main, Bias, Main+Bias	1, 2
0	650	0, 25	V_{ax}	Main, Bias, Main+Bias	1, 2
0	800	0, 25	V_{ax}	Main, Bias, Main+Bias	1, 2
100	50	0, 25	V_{ax}, m_{H2O} (no bias)	Main+Bias	1, 2
100	200	0, 25	V_{ax}, m_{H2O} (no bias)	Main+Bias	1, 2
100	350	0, 25	V_{ax}, m_{H2O} (no bias)	Main+Bias	1, 2
100	500	0, 25	V_{ax}, m_{H2O} (no bias)	Main+Bias	1, 2
100	650	0, 25	V_{ax} , m_{H2O} (no bias)	Main+Bias	1, 2
100	800	0, 25	V_{ax}, m_{H2O} (no bias)	Main+Bias	1, 2
300	200	0, 25	V_{ax}, m_{H2O} (no bias)	Main+Bias	1
300	350	0, 25	V_{ax}, m_{H2O} (no bias)	Main+Bias	1
300	500	0, 25	V_{ax}, m_{H2O} (no bias)	Main+Bias	1
300	650	0, 25	V_{ax} , m_{H2O} (no bias)	Main+Bias	1
300	800	0, 25	V_{ax}, m_{H2O} (no bias)	Main+Bias	1
		*MR- based on unbiased injector			
	1	bias injector near chamber wall, camera has back view of wall			
	2	both injectors equidistant from the wall, camera has back view of wall			

consisted of 10,153 images recorded at ~6688 frames per second. The cin-format file was first converted to 10,153 separate ASCII files. Since the subsequent image processing with POD was computationally intensive, the file size and number of frames analyzed were reduced. The time series was downsampled such that every 5th image was used for further analysis. This effectively reduced the frame rate by a factor of 5, or to

1,337.6 frames per second. Preliminary analysis confirmed that the frequencies in the sprays were much smaller (<50 Hz) and hence downsampling is not expected to have a major impact on the reported results. A reduced field of view (FOV) was chosen custom to each test condition such that this FOV included the most important regions of the spray, vis., the region near the injector and the spray-wall region. In order to account for spatial variation in background lighting, each spray image was subtracted from an image with no spray (background). The reduced field of view images were assembled into a single large Z_{nxm} matrix with dimensions corresponding to n times and m spatial locations,

$$Z_{nm} = \begin{bmatrix} z_{11} & z_{12} & \cdot & \cdot & \cdot & z_{1m} \\ z_{21} & z_{22} & \cdot & \cdot & \cdot & z_{2m} \\ \cdot & & & & & \cdot \\ \cdot & & & & & \cdot \\ \cdot & & & & & \cdot \\ z_{n1} & z_{n2} & \cdot & \cdot & \cdot & z_{nm} \end{bmatrix} \quad (1)$$

where z_{ij} correspond to intensity at pixel location i at time j. Proper Orthogonal Decomposition was performed using a singular value decomposition method as outlined in [3]. A singular value decomposition was performed on this matrix to yield three matrices, U, S and V.

$$Z_{nm} = U_{nn} S_{nn} V_{nm}{}^{t} \quad (2)$$

The matrix U consisted of the normalized expansion coefficients, the diagonal matrix S consisted of the square-root of the eigenvalues and the matrix V consisted of the eigenvectors of the decomposition. Eigenvectors are uncorrelated in space and expansion coefficients are uncorrelated in time. The original data can be recontructed as

$$z_{nm} = \sum_{j=1}^{N_{modes}} a_{nk} F_{km} \quad (3)$$

where a_{nk} constitute the elements of the expansion coefficient matrix, a projection of the original data onto aech eigenvector. Alternately, expansion coefficients can be evaluated by multiplying U with S.

After performing a POD, the spray data was typically reconstructed using the first 2 modes, the first 5 modes and the first 8 modes. For the lowest momentum-flux-ratio (MFR = 50), upto 50 modes were reconstructed. Typically, in excess of 98 percent of the spray core and its spread was described by the very first mode. The time variation of the spray was adequately expressed by less than 10 modes. However, over 300 modes were needed to reconstruct details of the smaller droplets outside the main spray core. Figure 4 presents POD reconstructions of a free-spray portion of the MFR 200 spray with the wall at 10 mm spacing. Shown in Fig. 4a is a snapshot of the original image, followed by reconstructions using 1, 30, and 300 modes in Figs. 4b, c, d and e respectively. Note that all figures are scaled from zero to unity.

The raw image sequence and POD reconstructions were then subjected to an image processing algorithm that involved edge detection and boundary tracing. The resultant images are shown in Figures 5a and 5b for a MFR of 200 and a wall spacing of 10 mm. Once the left and right spray boundaries were determined (Fig. 5a), a sixth order polynomial curve fit is drawn through the data at these boundaries. The polynomial curve fits were replotted in Figure 5b for all frames for the raw data along

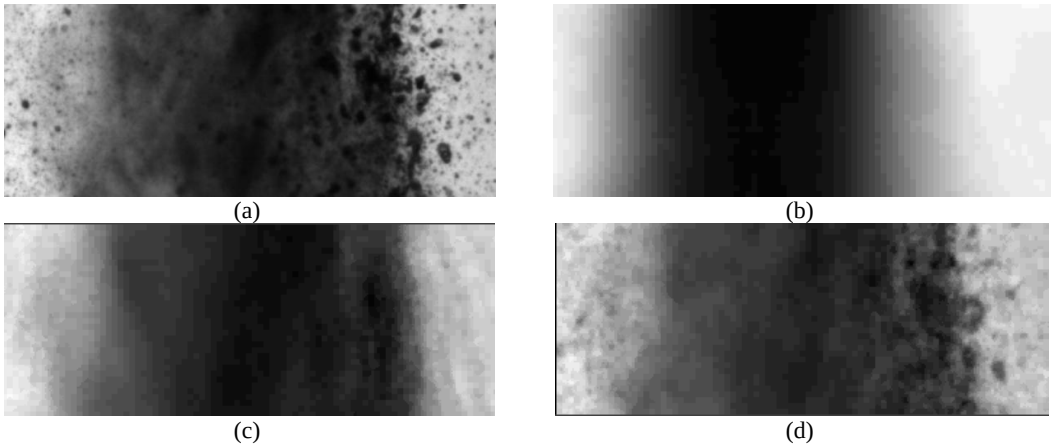

Fig. 4. Raw image compared against reconstructed images at t= 0 s. (a) raw image; reconstructions using (b) mode 1 , (c) modes 1-30, and (d) modes 1-300

with 2, 5, and 8 mode reconstructions. These polynomial were used to determine the spray width variation, attachment location, and the centerline deviations with time. A linear fit (blue line in Fig. 5a) was used to determine the spray angle variations. Once these data were determined, a Fast Fouruer Transform (FFT) was performed to determine the frequencies of left and right spray angle variation, centerline deviation, attachment location, and jet width variation at a chosen downstream location.

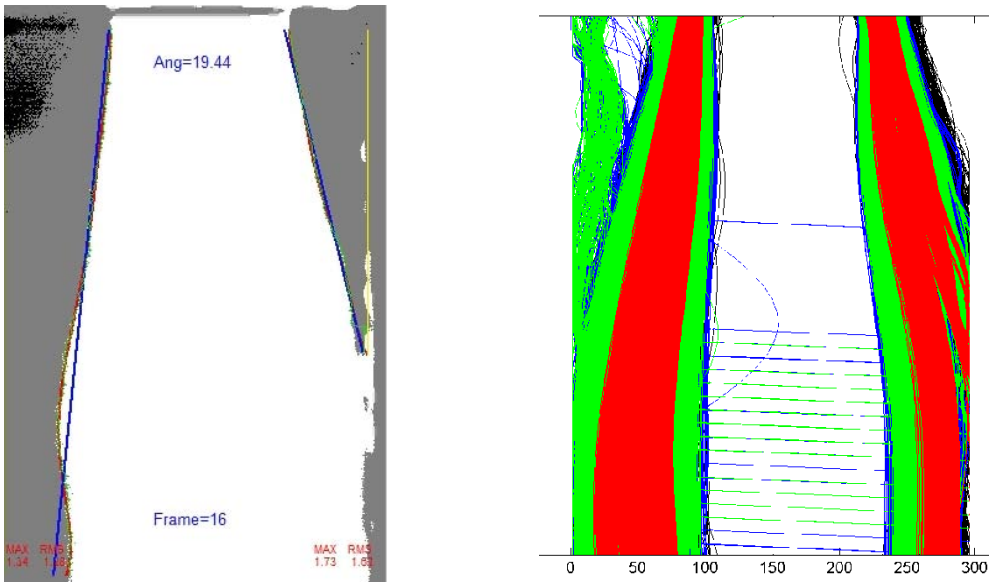

(a) (b)

Fig. 5. Post processing on reconstructed images for an MFR=200 spray. The injector is located 10 mm from the wall (a) binarization (b) spray edge detection for raw (black), and reconstructions using modes 1-2 (red), modes 1-5 (green, and modes 1-8 (blue)

Figure 6 shows results of left and right spray angles for a MFR 200 spray with the injector located 10 mm from the side wall. Figure 6a shows the spray angles determined using the raw intensity plots while Figs. 6b and 6c shows the angles determined using reconstructions of modes 1-2 and modes 1-8 respectively. Figure 6d shows a frequency plot of spray angles determined from all three time series plots. From each of the time series plots in Figs. 6a-c, it is clear that the left and right spray angles show cyclic variations and are out of phase with each other, which is indicative of a swaying motion

of the spray. The 2 mode reconstruction in Fig. 6b seems to lock onto particular locations at the wall which causes the right angle to remain fairly constant over half a period of the cycle. The eight mode reconstruction does not show this behavior and is closer to representing the raw data variations. The FFT plot on Fig. 6d indicates distinctly strong peaks for the 5 and 8 mode reconstructions indicating that these reconstructions extract the dominant frequencies in the data while mitigating the noisy data. The dominant frequencies are represented by all modal reconstructions indicating that a 2 mode reconstruction is probably sufficient to determine the low frequency content in the spray.

The time series variation attachment location is presented in Fig. 7 for MFR of

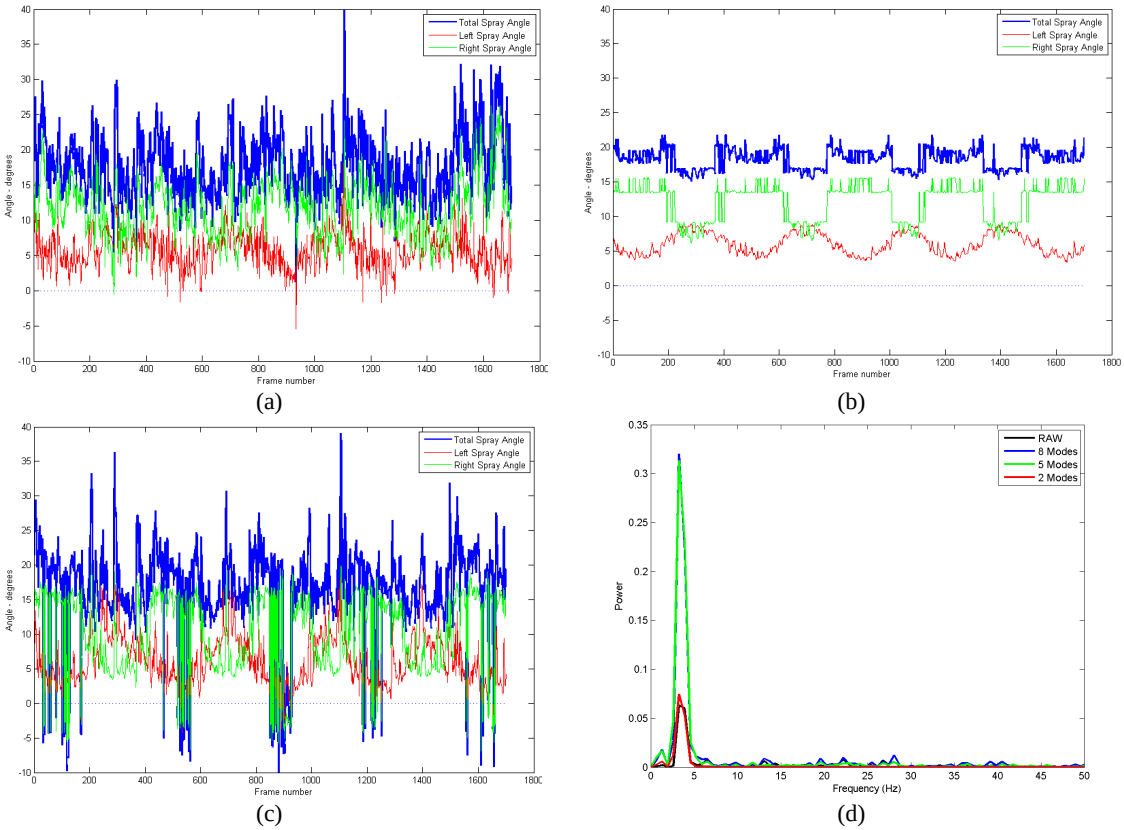

Fig. 6. Spray angles for the MFR=200 spray with wall located 10 mm away from the injector edge. (a) raw image, (b) modes 1-2, (c) modes 1-8, and (d) power spectrum plot for raw, modes 1-2, 1-5, and 1-8.

200 and 800. Both sprays are at a wall spacing of 5 mm. A large variation of nearly 80 pixels in reattachment pixel location is evident for the MFR 200 spray. The location varies at a frequency of approximately four hertz. The variation in attachment location for MFR 800 spray is much less significant at approximately 30 pixels.

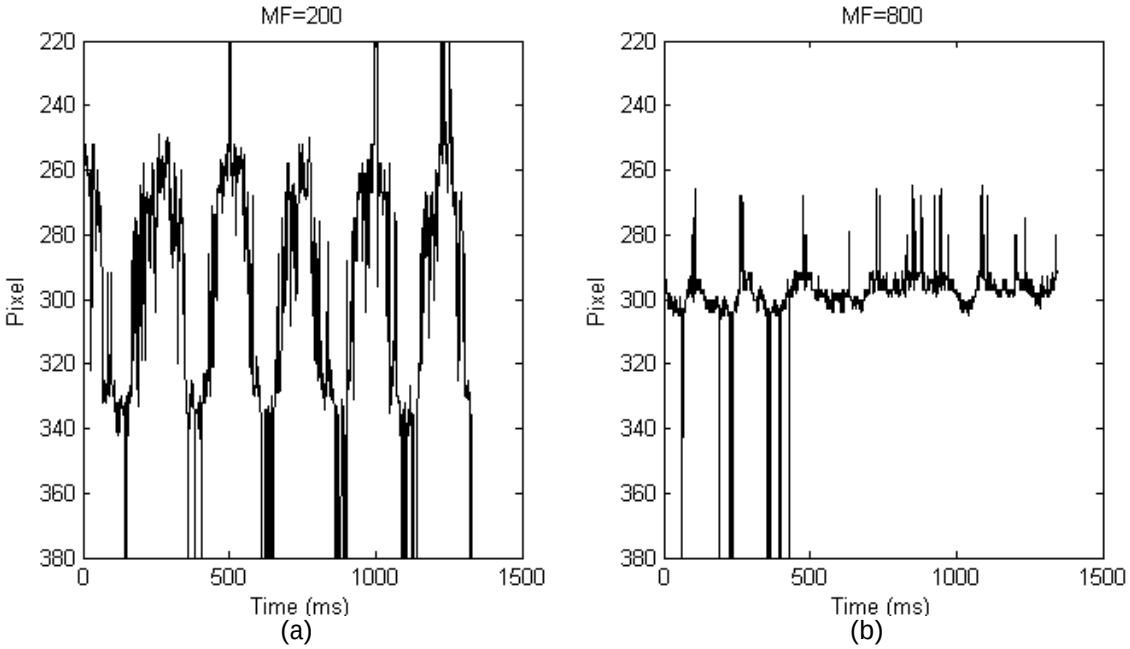

Fig. 7. Variation of attachment location with time for (a) MFR = 200 and (b) MFR = 800. The wall is at 5 mm from the injector edge.

Intensity fluctuations were also analyzed using the POD method over a small field of view close to the injector as shown in Fig. 8a. For this analysis, the instantaneous intensities at each spatial location was subtracted from the spatially local time-mean value to yield an intensity flutuation data matrix. This matrix was then subjected to POD and data from different modes were reconstructed. The first mode accounted for 15 percent, the first 10 modes accounted for 55 percent, and the first 100 modes accounted for 84 percent, of the variations in the data. Figure 8b presents the expansion coefficients, defined in Eq. 3, for the first five eigenvectors. These expansion coefficients

are determined from the singular value decomosition by a multiplication of the first two matrices on the right side of Eq. 2. The coefficients are normalized by the corresponding eigenvalues of each mode. Most of the expansion coefficients had a dominant peak at approximately 6 Hz. This frequency correlated well with the frequency of the jet obtained from the raw intensity images, indicating that it was related to the swaying of the jet.

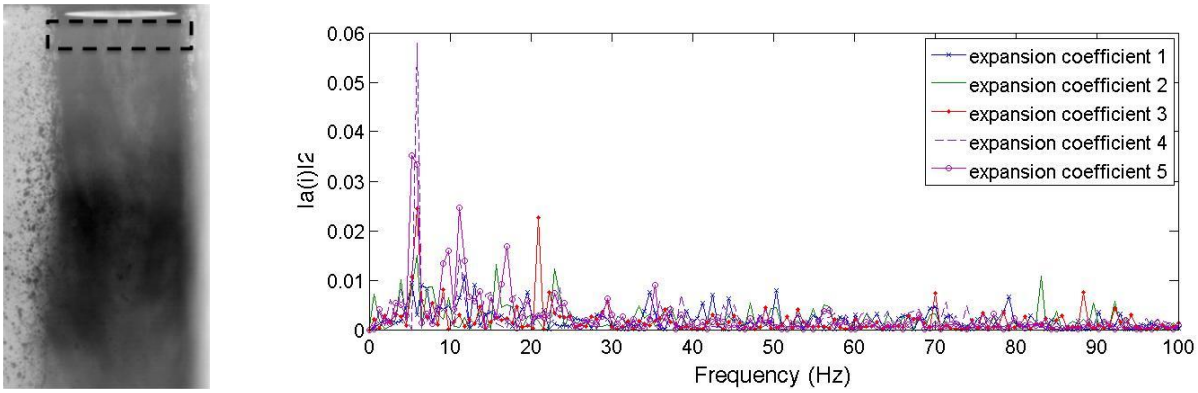

Fig. 8. POD on fluctuating intensity time series. (a) location of analyzed field of view relative to the spray extent, (b) expansion coefficients of the first five eigenvectors.

Conclusions

Injector-wall interaction was studied experimentally using high-speed imaging for gas centered swirl coaxial injectors. Three sets of experiments were performed- the first with a single injector and a side wall, the second set with two injectors and one side wall and the third set with two injectors located within the chamber.

A POD method of data analysis was employed to analyze time series of raw and fluctuating intensity images. For the raw intensity images, the first 2 modes typically captured the variation of the mean spray angles and attachment points with time. A significantly higher number of modes were required to reconstruct the time series of fluctuating intensities. Larger variations in wall attachment locations were observed for

the MFR 200 spray compared with the MFR 800 spray. In general, the wall dampens the spread of the wall-bounded spray.

References

1. Lightfoot, M. D. A., Clark, K. A., Danczyk, S. A., Lyu, H. S., Talley, D. G., 2008, "Film Behavior in Gas-Centered Swirl-Coaxial Injectors," Proceedings of the 55th JANNAF/ 4th LPS/ 3rd SPS/ 6th MSS Joint Meeting, Orlando, Florida.
2. Lightfoot, M. D. A., Danczyk, S. A., Talley, D. G., 2008 "Scaling of Gas-Centered Swirl-Coaxial Injectors," Proceedings of the 55th JANNAF/ 4th LPS/ 3rd SPS/ 6th MSS Joint Meeting, Orlando, Florida.
3. Holmes, P., Lumley, J., and Berkooz, G., 1996, *Turbulence, Coherent Structures, Dynamical Systems, and Symmetry*, Cambridge University Press, Cambridge, UK.